AIAA SciTech
5-9 January 2015, Kissimmee, Florida
56th AIAA/ASCE/AHS/ASC Structures, Structural Dynamics, and Materials Conference

Topology Optimization of Additively-Manufactured, Lattice-Reinforced Penetrative Warheads

Hayden K. Richards[1] and David Liu[2]
Air Force Institute of Technology, Wright-Patterson AFB, OH, 45433

Two different scaled penetrative warheads were developed using additive manufacturing processes in 15-5 stainless steel. The first warhead design had a singular unitary case based solely on existing penetrating warhead designs. The second warhead design was a modification of the first, where the nature and location of new internal members and lattice structures was determined using topology optimization methods. The relative physical properties of the two warheads were calculated using HyperWorks, a commercial finite element analysis software. Once these analyses were finalized, production of the warheads was accomplished using direct metal laser sintering. The two warheads will be live-fire tested at Eglin AFB, FL. The analysis and physical testing will validate the ability of additively manufactured warheads to penetrate targets, the ability of lattice structures to perform well in impact loading environments, and the utility of topology optimization methods for warhead design.

Nomenclature

cm	=	centimeter
in	=	inch
mm	=	millimeter

I. Introduction

Penetrative warheads, characterized by massive, strong, and tough solid cylindrical cases with ogive noses, are generally manufactured using traditional techniques such as subtractive fabrication processes.[1] In these processes, material is removed from pre-formed solid masses to produce simple shapes. Recently, the development of sophisticated additive manufacturing (AM) machines, known colloquially as 3D printers, has revolutionized the process of building metal parts.[2] AM machines are capable of producing extremely complex shapes in a variety of materials with high accuracy, tight tolerances, and good consistency. [3]

This paper explores the capabilities of AM in building penetrative warheads with certain physical, structural, and performance characteristics. The primary goal of this research was to maintain penetrative performance of a warhead while reducing the thickness of a penetrating warhead case wall. This was accomplished through the use of additive manufacturing and the application of two research disciplines. First was the use of lattice structures as load bearing elements. Lattice structures, examples of which are shown in Figure 1, were used to generate structures with specific material properties. In this research, different material properties, and therefore different structure physical responses, were generated by careful tailoring of the design and application of lattice structures.[4,5] Additive manufacturing is preferred to produce complex lattice structures, as the use of traditional manufacturing methods is extremely difficult and expensive.[6] The second research direction was the use of topology optimization as a design tool. Topology optimization is the process of finding the ideal distribution of material within a structure.[7] In practice, topology optimization, when applied to some design space under a user-defined loading condition, returns a density gradient of the material within the design space, optimized to the desired specifications.

Through the use of AM and the appropriate application of lattice structures and topology optimization, a simple penetrating warhead was designed and optimized for loading conditions consistent with a penetration event. In order to verify the improvement of the optimized warhead, penetrating tests were conducted at Eglin Air Force Base (AFB), Florida (FL).

[1] Masters Student, Department of Aeronautical and Astronautical Engineering, Student Member AIAA
[2] Assistant Professor, Department of Aeronautical and Astronautical Engineering, Senior Member AIAA

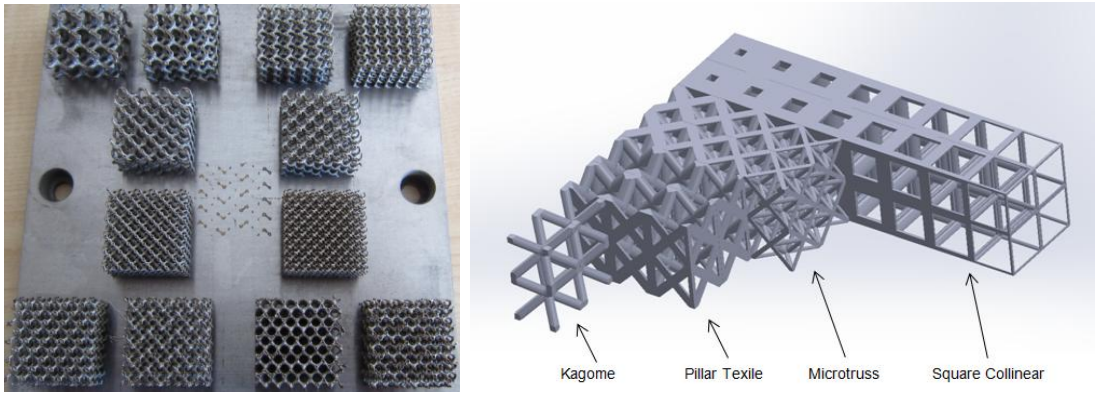

(a) (b)

Figure 1. Lattice Structures. (*a) Examples of different lattice structures produced using additive manufacturing of 316L stainless steel.*[4] *(b) Lattice structure examples generated for this research.*

II. Methodology

Two different penetrating warhead designs were developed in the course of this research. The first, dubbed the *standard* warhead, was designed based on existing penetrating warhead geometries. The second warhead, dubbed the *optimized* warhead, was created by modifying the standard design to match the geometry generated by topology optimizations.

The two designs were applied to warhead shapes provided by the Munitions Directorate, Air Force Research Laboratory at Eglin AFB, FL. During the course of this research the warhead shape was changed from the one shown in Figure 2(a) to the one shown in Figure 2(b) to improve penetration performance. The first shape has a Caliber Radius Head (CRH) of 1.0 and the second a CRH of 4.5. Both shapes have an outer diameter of 1.0 in and length-to-diameter ratio of 7.5. These dimensions were selected to ensure the warheads would fit in the build volume of the EOS M270-M280 series of 3D printers, which are capable of 3D printing in a variety of stainless steels such as the EOS StainlessSteel PH1 used for this work.[8] This steel is equivalent to 15-5 stainless steel defined by standard UNS 15500.

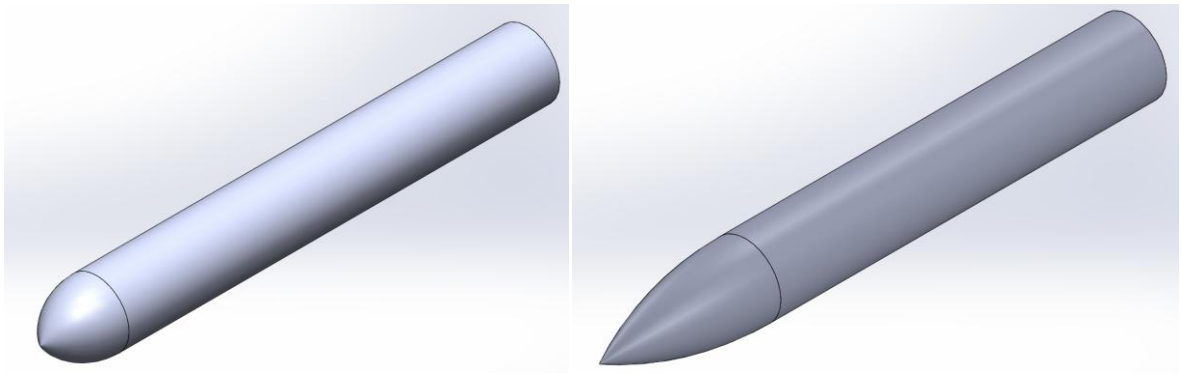

(a) (b)

Figure 2. Penetrating Warheads. *(a) Standard warhead design, CRH = 1.0 shape (b) Standard warhead design, CRH = 4.5 shape*

Design of the new optimized warhead was subject to certain constraints. Most restrictively, consistency of the shape, size, and overall weight of all tested warheads was required. This restriction meant only the internal structures of the standard warhead were modified in the optimized design. In addition, minimization of the wall thickness of the optimized warhead was desired in order to improve the fragmentation characteristics of the warhead. The optimization was performed to reduce case wall thickness while maintaining overall penetrative capability.

The approach taken was to remove the inner 50% of the warhead case wall by thickness and redesignate this mass as available design mass. This mass became open to redistribution within the new larger case interior. Figure 3 shows the difference between the original 3D case and the new thinner 3D case with the internal design space shown in blue. The topology optimization program used the redesignated available mass for its operation and conserved overall warhead mass and volume by ensuring the mass occupying the blue design volume weighed as much as the mass which was removed to reduce the wall thickness. In practice, however, volume was conserved. The standard warhead shown in Figure 3(a) had a case wall volume of 36.42 cm^3 and enclosed an internal cavity volume of 47.96 cm^3. The 50% thick case wall shown in Figure 3(b) had a volume of 20.47 cm^3 and enclosed an internal cavity of 63.90 cm^3. The difference in actual case volume between these designs was 15.94 cm^3 which, when redistributed within the interior of the 50% thick case, filled it to a volume fraction of 24.95%. Table 1 outlines these values.

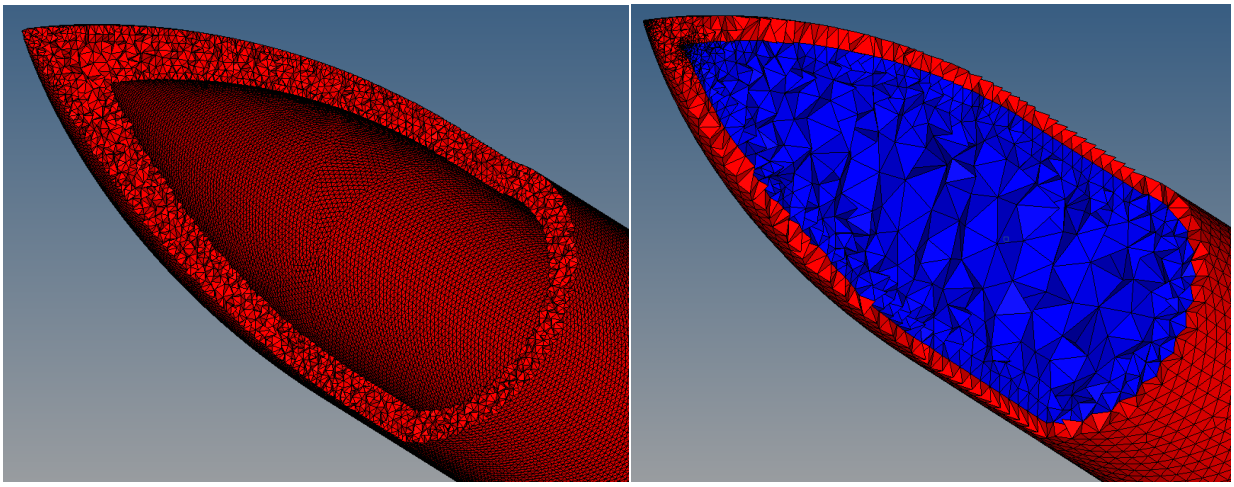

(a) (b)

Figure 3. Design Details. *(a) Case wall thickness at the warhead nose for the standard design. (b) Case wall thickness of the optimized design. Note the internal design volume available in the optimized case. For both cases, an adaptive mesh was used for finite element analysis. The fully thick warhead has an average element length of 0.050 cm while the 50% thick warhead has an average element length of 0.100 cm. Red represents non-design regions and blue represents design regions. During optimization runs, only design regions were assigned as design variables.*

Table 1. Design Modification & Volume Parameters. *Outline of material volume allocation (calculated in Solidworks 2013).*

Item Identification	
Standard full thick case wall volume	36.42 cm^3
Standard full thick interior cavity volume	47.96 cm^3
50% thick case wall volume	20.47 cm^3
50% thick interior cavity volume	63.90 cm^3
Case wall difference (available material volume used by HyperWorks for optimization)	15.94 cm^3
Volume fraction required for 50% interior cavity to ensure mass & volume conservation	24.95%

HyperWorks was used for both finite element analysis and topology optimization. HyperWorks is a family of computer-aided engineering simulation software tools. The HyperMesh program was the primary tool within HyperWorks used for component meshing, load application, and optimization definition. Optistruct was the software used for analysis and optimization generation, and HyperView was the result viewing tool.

Once the standard warhead was modeled in HyperMesh, different load and constraint conditions were applied. Since the exact loading conditions expected under penetrating impact are difficult to measure, representative loads were applied to the model. Although these representative loads did not directly predict the penetrating performance of the warhead, they allowed for relative behavioral comparisons between the standard design and the subsequent multiple different optimized designs over time. Several different loading conditions were defined, including axial, bending, and offset angular loads, body forces, and different constraint locations and settings. In addition, some loading conditions were applied to two-dimensional (2D) slices of the warhead case to reduce complexity and shorten computational time. Examples of both 2D and three-dimensional (3D) results are presented in this work.

After a wide range of loading conditions were applied to the standard warhead model, the optimized design was modeled separately and the same or equivalent loading conditions were applied. Optimization was then performed on the model using the applied loading conditions. A variety of different optimization parameters were used with the exception of the volume fraction constraint. This was fixed at the required value in order to guarantee a fixed overall mass.

Finally, an optimized result from HyperWorks was used to generate an optimized warhead design. This was performed in a variety of ways. All actual design work was accomplished via Computer Aided Design (CAD) using Solidworks 2013. Designs generated from 2D optimizations solutions were produced by revolving the optimized solution about the central axis, producing a 3D solid. This solid was then modified with the incorporation of longitudinal channels, the addition of lattice structures, and other modifications required to ensure printability. Designs generated from 3D optimization solutions did not require revolution. The other modifications, however, were still required to ensure design printability.

The actual optimized design selected for production was the best design produced throughout the multiple optimization trials. It was selected based on many different quantitative and qualitative factors. One quantitative factor included was total case displacement in the longitudinal direction. The displacement of the optimized case was compared to the displacement of the standard case under the loading conditions of the optimization. It was desired for the optimized case to displace less than the standard case. Total case displacement of the optimized case compared to the standard case was also considered for different loading conditions than used for the optimization. Another quantitative factor was actual optimization response values such as total compliance of the warhead models. Qualitative factors were considered as well. These included optimization solution quality, HyperWorks-to-Solidworks transition convenience, lattice structure integration considerations, and printability. Optimization solution quality is defined and discussed in section III.C. HyperWorks-to-Solidworks design convenience relates to the complexity of the optimization solution and the level of detail and effort required to produce the equivalent Solidworks design. Lattice structures were used within regions of moderate density within the optimization, which certain optimization solutions contained. Printability encompasses a wide range of concerns, both materialistic and geometric, which govern what the M270-280 series of 3D printers are capable of producing.

Upon the finalization of the optimized design, both designs were printed in EOS StainlessSteel PH1 using EOS M270 and M280 Direct Metal Laser Sintering (DMLS) machines. They will be tested for penetration performance in live-fire testing at Eglin AFB, FL in January 2015. For each different penetration test a traditionally manufactured warhead produced in ‘Eglin steel’ will also be tested in addition to the standard and optimized additively manufactured designs. This will allow comparison between the additively manufactured warheads and the traditional unitary design. Eglin steel is a propriety stainless steel alloy developed by the Munitions Directorate for warhead cases.

III. Results and Discussion

Five different sections are presented below representing the results and discussion of this research. Initially, a preliminary test warhead was printed using DMLS processes to test the ability of 3D printing to produce penetrating warhead shapes. In addition, a simple analysis and optimization was carried out to verify the relative performance between standard and optimized warhead designs. Once the optimization routine was confirmed to generate quality solutions, more in-depth optimizations were conducted. Structural analysis was then performed on the standard warhead case wall under set loading conditions. This provided a set of loading condition for comparison of various topology optimized solutions. Next, the same loading conditions were applied to the 50% thick case to determine the optimization solution with the thinner wall condition. The optimization solution was translated into a completed final design. Lastly, the final design was prepared for DLMS and tested for performance against concrete targets.

A. Preliminary Warhead

A preliminary warhead with the CRH = 1.0 shape and the standard design was printed early in the research process to explore the ability of the DMLS process to match specified tolerances and print the desired ogive shape for the nose cone. The warhead was printed in a 'laying down' build orientation, and is shown in Figure 4. Table 2 outlines some differences between expected and produced dimensions. Per manufacturer specifications, the EOS M280 machine which printed the initial warhead should have a dimensional tolerance of ± 20-50 µm.[8]

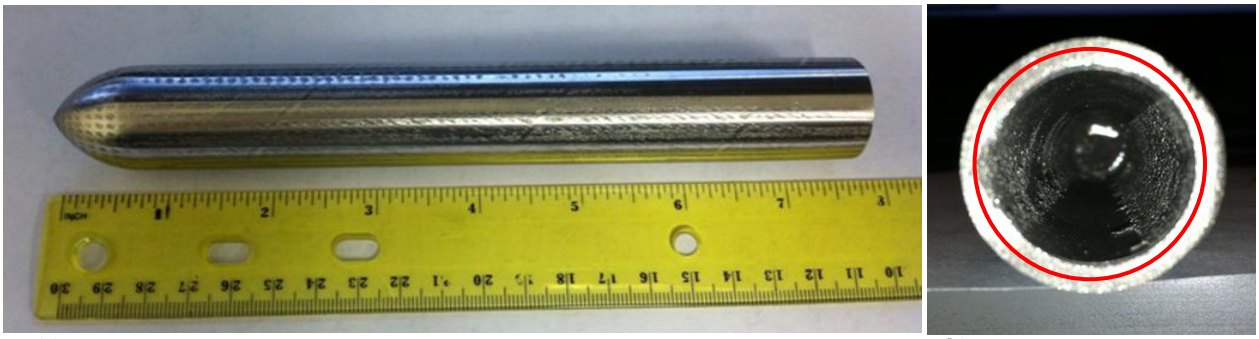

(a) (b)

Figure 4. Preliminary Warhead, CRH = 1.0 shape. *(a) Initial warhead prototype, side view. Warhead length = 7.5 in. Surface finish was shot peened and brushed. (b) Initial prototype, back view. Radius = 1.0 in. Note the CRH = 1.0 warhead shape. Red circle is exact with radius = 0.9 in. It helps to demonstrate the slightly out-of-round nature of the printed warhead.*

As Figure 4 and Table 2 shows, the preliminary test warhead demonstrated some significant concerns about the DMLS process. All dimensions were outside the expected tolerances, and the overall shape was "out-of-round" as illustrated in Figure 4(b). In order to address these concerns, several changes were made to the printing standards used for subsequent builds. First, all subsequent warheads were produced "standing up" with the longitudinal axis of the warhead oriented in the vertical direction. Second, a thin layer of grind stock was added to the outside of the warhead. This stock was subsequently removed post-printing by traditional manufacturing processes. This ensured the outside dimensions of the warhead matched exactly the desired design shape. All together, these changes produced higher quality parts for all further warheads.

Table 2. Preliminary Warhead Specifications. *A comparison of expected tolerances and actual design dimensions for the preliminary warhead. In order to calculate the values in the actual vs. tolerance column, the maximum change from design to actual dimension was determined and compared to the maximum expected tolerance of 50 µm. Max tolerance = 50 µm.*

Measurement	Machine Tolerance	Dimension as Designed	Actual Dimension Produced	Actual vs. Tolerance
Diameter	± 20-50 µm	1.00 ± machine tol. in	1.00 ± 0.011 in	5.5× max tolerance
Length	± 20-50 µm	7.55 ± machine tol. in	7.55 ± 0.010 in	5× max tolerance
Wall Thickness	± 20-50 µm	0.11 ± machine tol. in	0.123 ± 0.003 in	8× max tolerance
Weight	-	292 g ± 5 g	315 g (+23 g)	7.8% error

B. Performance Comparison & Optimization Validation

A simple analysis was completed to compare the performance of the optimized design to the performance of the standard design. For this analysis, performance was defined as case displacement in the longitudinal direction under axial loading. Both the standard and optimized models were subjected to a loading consisting of constraints at the tail and an axial load applied at the tip, as shown in Figure 5. A topology optimization was then performed in HyperWorks. The optimized design, shown in Figure 5(a), is compared to the standard design shown in Figure 5(b) where the color gradients represent material density. The longitudinal displacements for both the optimized design, depicted in Figure 6(a), and the standard design, shown in Figure 6(b), are presented. In comparing Figure 6(a) and 6(b), the optimized design displaced 0.0623 cm at the tip while the standard design displaced 0.0957 cm, resulting in a 34% decrease in displacement at the tip of the warhead for the optimized case. In addition, lateral displacement is also a concern under impact conditions for penetrating warheads. According to penetration testing experts at the Munitions Directorate, a weakness to lateral displacement can cause the tip of an impacting warhead to mushroom and collapse in on itself rather than penetrate the target. In Figure 6, arrows show the location of the maximum lateral displacement on each design. At their respective maximum-displacement locations, the optimized warhead displaced laterally by 0.0365 cm and the standard warhead by 0.342 cm. Not only did the optimized warhead displace about $1/10^{th}$ as much as the standard warhead, the location of maximum displacement was farther aft on the optimized warhead.

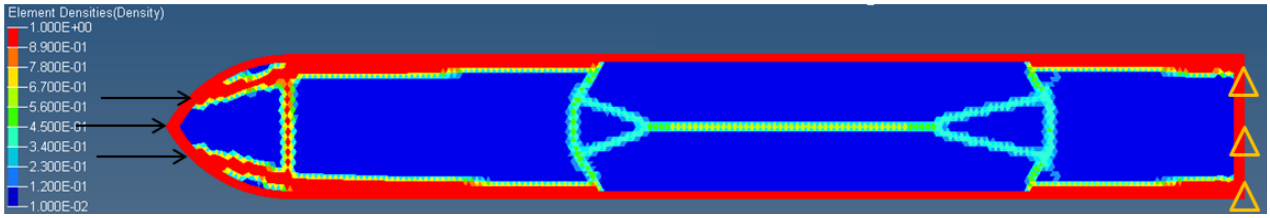

(a)

(b)

Figure 5. Optimized vs. Standard Design. *(a) Optimized design. (b) Standard design. Color gradients in both designs reflect density gradients, with red elements being 100% dense and blue elements 0.01% dense.*

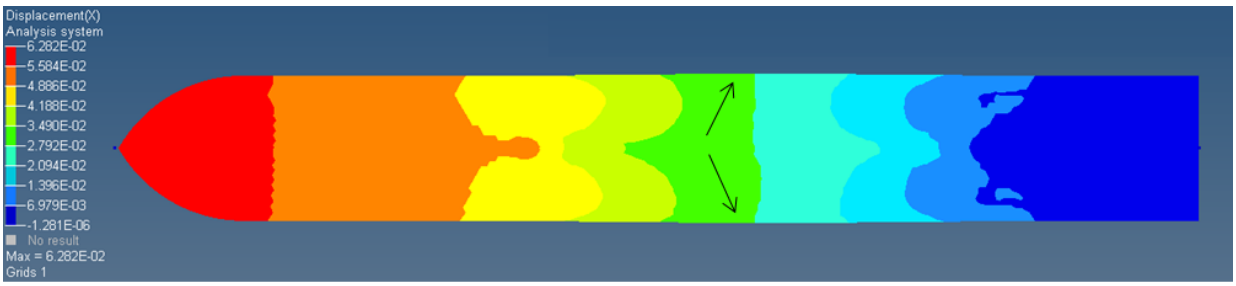

(a)

(b)

Figure 6. Optimized vs. Standard Design, Longitudinal Displacement (cm). *(a) Longitudinal displacement of optimized warhead design. (b) Longitudinal displacement of standard design. Axial loading condition applied to both models. Arrows highlight location of maximum lateral displacement.*

C. Analysis & Optimization

Additional optimizations were completed on both 2D and 3D warhead models under various loading conditions. Several of them are for the previously described preliminary warhead nose shape with CRH = 1.0, which was subsequently modified to the testable design with CRH = 4.5.

Topology optimizations produce material density gradients within the design. The optimization process was controlled through the manipulation of five unique control inputs. These were design variable(s), responses, constraints, objective, and additional parameters. Design variables govern the elements the optimization routine considers for density variation. For this research, the internal area and volume were used exclusively as the design variables for 2D and 3D analyses, respectively. These internal elements were designated as having the design property allowing the topology optimization routine to vary their densities. Responses define measurements the optimization routine can use such as compliance, volume fraction, displacement, stress, strain, etc. Responses defined in the examples for this research were total compliance and volume fraction of the internal area or volume. Constraints are limitations imposed on any individual response and must be maintained during the optimization process. For example, the 3D optimizations presented here were constrained to an internal volume fraction of between 0.245 and 0.255 forcing the internal volume fraction towards the 24.95% desired. The objective defines the desired property. Objectives are generally either maximized or minimized and are the single items having the most control over the outcome of the optimization. All examples in this work minimized total compliance to ensure maximum stiffness. Finally, additional parameters allow for further control on the optimization routine such as member size, pattern groupings, or draw directions. Member size controls, utilized in some of the designs, force single truss members to have widths within a given range. For example, the user can choose to regulate member sizes to between 0.25 cm and 0.5 cm.

Once these five inputs were determined, the last parameter left to define for the optimization was the loading condition, referred to as the "loadstep". Many different loadsteps were applied to several optimization runs. For simplicity, the different loading conditions were defined by descriptive names. These loadstep definitions were the same for both 2D and 3D models. Body loadsteps refer to loads applied to the entire case wall and evenly distributed over all element nodes. Loads of 1.0 N were applied for the standard 0.050 cm element size. For the 0.100 element size, the loads were scaled according to the number of nodes so the total load applied was the same. The body-axial loadstep had compressive axial loads applied in the longitudinal direction, while the body-angle loadstep had the compressive body loads applied at a 20º offset angle. An illustration of the loadsteps is shown in Figures 7 and 8 where the yellow triangles represent constraints and the black arrows represent the loads applied to the design. For all body loadsteps, constraints were applied at the tip of the warhead, with 45 nodes being constrained in 2D models and 83 nodes constrained in 3D models. The constraints were applied for all six degrees of freedom at each node.

Figure 7 and Figure 8 illustrate a small subset of the optimization results generated during many optimization runs. The examples in these figures were chosen to reflect the nature of the optimizations and represent a variety of different results based on the loadsteps. For reference, Table 3 outlines the different optimizations depicted in the two figures.

When analyzing the quality of optimization results, certain characteristics stand out. In general, quality optimizations are defined in this research as optimization results with clear distinction between high-density and low-density regions, obvious structural elements, single interconnected bodies, and designs for which good performance under impact and penetration was expected. Poor quality optimizations were characterized by disconnected or isolated material concentrations, dangling structural elements, significant regions of moderate density, and weak expected performance against impact. The following paragraphs analyze some of the strengths and weaknesses of the optimization results shown in Figures 7 and 8.

Figure 7(a) was one of the first quality optimizations generated with the CRH = 1.0 warhead shape. The model was subject to body-angle loadstep and the internal volume fraction was constrained between 0.25 and 0.50. Qualities of this optimization include the very clear distinctions between high-density and low-density elements and the well-defined truss structure. Weaknesses of this optimization include the thin member sizes towards the rear of the warheads, the hollow tip, and the thick wall. Despite these drawbacks, this optimization was used as a basis for the finished design presented in section III.D.

Figure 7(b) is an early optimization result for the CRH = 4.5 warhead shape. It was also a body-angle loadstep, the volume fraction was restricted to between 0.2 cm and 0.3 cm, and no additional parameters were applied. The resulting optimization is characteristic of results with these inputs. Although the warhead appears improved for penetration with its thick tip, overall the optimization is poor since has a poorly-resolved center section and several

unfinished internal trusses. Additional resolution and optimization control was required to resolve the structure, producing the desired result as shown in Figure 7(c).

Figure 7(c) is the result of additional controls applied to the optimization used to generate Figure 7(b). It has the same optimization parameters, with the addition of member size control between 0.5 cm and 1.0 cm. As a result, the members are more defined when compared to previous optimizations. The truss elements are distinct, there are fewer moderate-density regions, and the wall thickness is reduced. Unfortunately, the tip is still slightly hollow and the design could still use some further resolution. Despite these concerns, this optimization result has potential for use to generate a finished design. The parallels in shape and truss pattern between this solution and the solution in Figure 7(a) are expected considering the similarities between the respective optimization inputs.

Figure 8(a) is an early 3D optimization of the CRH = 1.0 warhead shape. Using a body-axial loadstep, this optimization enforced the tight volume fraction constraint between 0.245 and 0.255 in addition to enforcing 8-point cyclical symmetry. The effect of the symmetry control is seen towards the back of the optimization solution. The three small points of higher-density mass are three of the eight points which appear around the entire case. Very little material is generated along the central axis of the warhead body cylinder, yielding thick walls which are undesirable for this effort. Nevertheless, this optimization does have a favorable forward weight distribution for aerodynamic stability purposes. This optimization, however, has very little material towards the tail of the warhead to resist bending which may allow for undesirable tail-slapping during impact.

In Figure 8(b), the loadstep was changed to body-angle with little change to the result when compared to the result in Figure 8(a). The cyclical symmetry parameter was removed and replaced by member size control, which did not have a significant effect on the result. The volume fraction constraint was further constrained to between 0.249 and 0.250. Although this solution has the desired forward volume distribution, the rationale for the asymmetry and void locations remain unclear at this time and may result from poorly suited input parameters. This solution has less material in the tail when compared to the result shown in Figure 8(a).

Taken together, these optimization results allowed for several conclusions. First, the results showed the diversity of expected optimization solutions based on inputs. The nature of the optimized solution set depended heavily on the inputs which must be well-posed to generated acceptable solutions. Examples of inputs which caused significant optimization variability are the objective, loadstep, and member size control. Second, the results show the differences found between 2D and 3D optimizations. Figures 7(c) and 8(b) are one example of this. They are approximately the same optimization performed on 2D and 3D models. Despite the desire to use 3D results, the higher fidelity 2D results formed the basis for many successful optimizations and the subsequent final designs. The 2D optimizations were also easier to perform because, compared to 3D, they were less computationally intensive resulting in less computational time. Finally, the topology optimization motivated the insertion of lattice structures. Certain optimizations, such as the optimization shown in Figure 7(c), were more suitable to the insertion of lattice structures since the distinct areas of moderate-density elements provide locations in which lattice structures provide the desired moderate physical and structural properties. This optimization is particular offered both clear trusses and areas of medium density. These locations of moderate density were the ideal location for the insertion of lattice structures to support solid trusses. These considerations were all taken into account when designing the final warhead.

Table 3. Optimization Result Review.

Fig #	Design Variable	Constraint(s)	Objective	Loadstep	Additional Parameters	Comments
7(a)	Interior Area	Volume fraction ϵ (0.2,0.5)	Min. total compliance	Body-angle	Min/max member size (0.25,0.5)	2D design basis
7(b)	Interior Area	Volume fraction ϵ (0.2,0.3)	Min. total compliance	Body-angle	-none-	
7(c)	Interior Area	Volume fraction ϵ (0.2,0.3)	Min. total compliance	Body-angle	Min/max member size (0.5,1.0)	Same as 7(b) w/ member size
8(a)	Interior Volume	Volume fraction ϵ (0.245,0.255)	Min. total compliance	Body-axial	Cyclic pattern grouping 8x	
8(b)	Interior Volume	Volume fraction ϵ (0.249,0.250)	Min. total compliance	Body-angle	Min/max member size (0.5,1.0)	

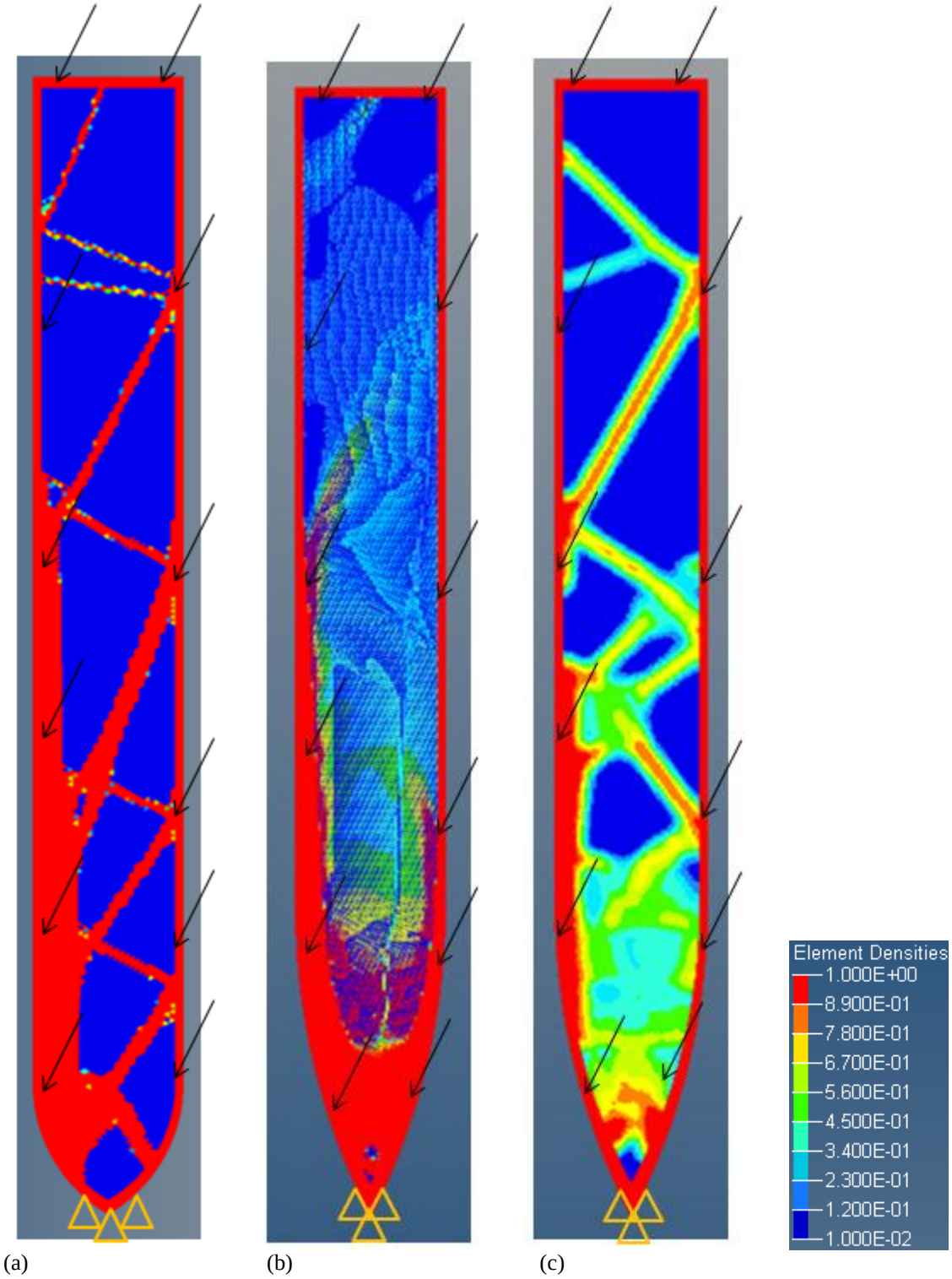

Figure 7. 2D Warhead Optimizations. *(a) 2D angle loadstep optimization. (b) 2D body-angle loadstep optimization. (c) 2D body-angle loadstep optimization. This optimization is the same as the one in Figure 7(b) with the addition of member size control.*

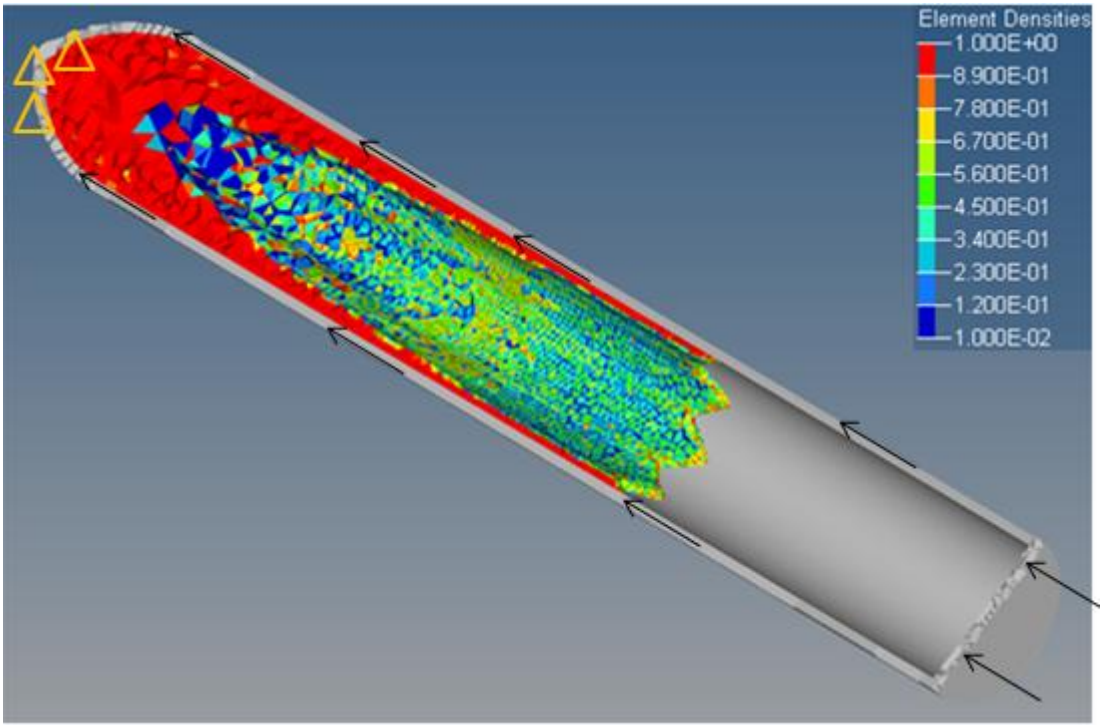

(a)

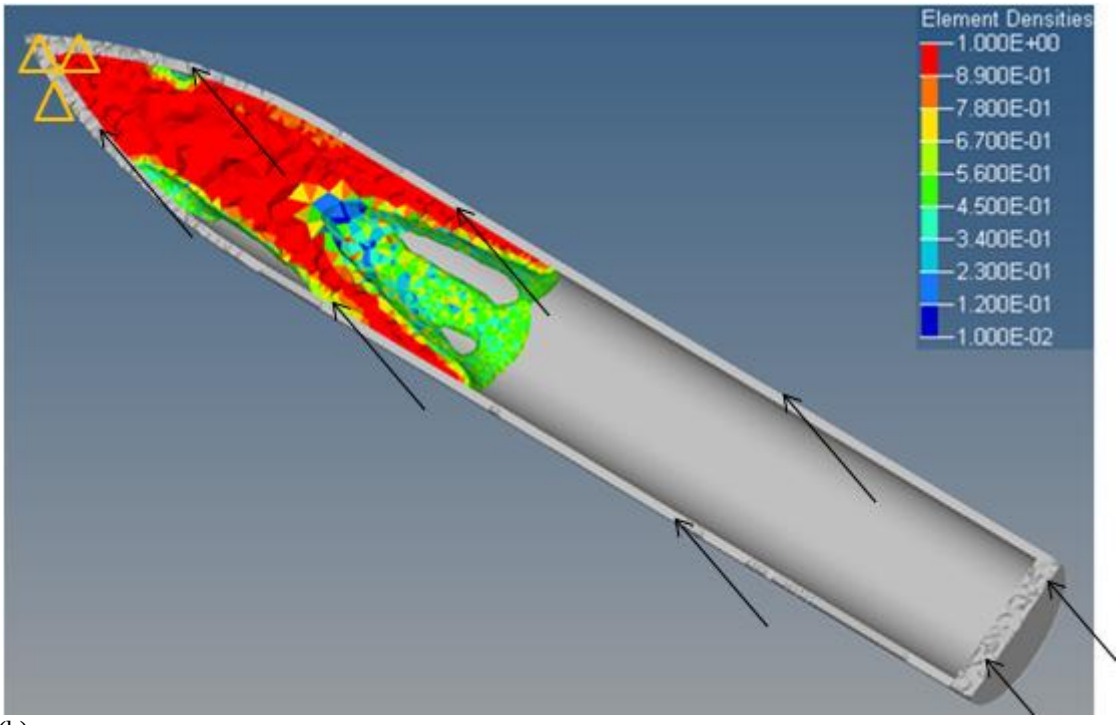

(b)

Figure 8. 3D Warhead Optimizations. *(a) 3D body-axial loadstep optimization. (b) 3D body-angle loadstep optimization.*

D. Finished Design

The optimization result shown in Figure 7(a) provided the basis for the optimized warhead design shown in Figure 9. Although this example is not the actual warhead expected for testing, it represents the process used to translate the optimized results into a printable warhead design. As this research is ongoing, the finalized design for testing will be presented at a later time. Since the optimization was in completed in 2D, a revolution about the longitudinal axis was required to produce a 3D part. This revolution was performed in Solidworks, and solid members were based on the high-density elements of the optimization. The resulting solid was then perforated by eight longitudinal channels to provide for metal powder removal after the DLMS building process. Furthermore, the longitudinal perforations also helped to maintain thin case walls and reduce the total weight of the warhead to the desired quantity. This stage of the design is illustrated in Figure 9(a). As a result of structural material removal, lattice structures were added to increase overall strength, support the solid elements, and fine-tune the overall warhead mass. The addition of lattice structures is shown in Figure 9(b).

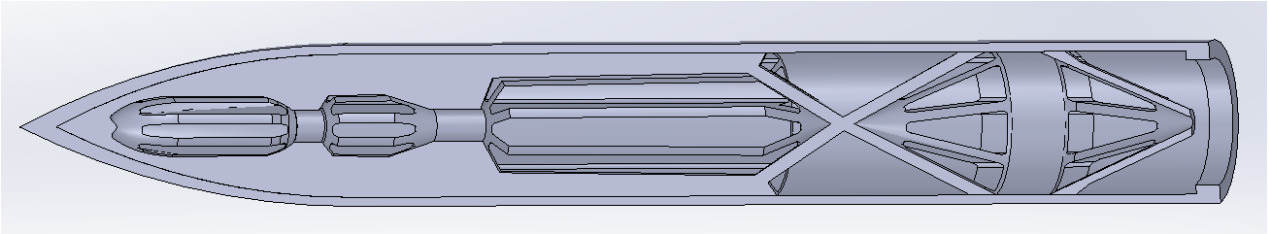

(a)

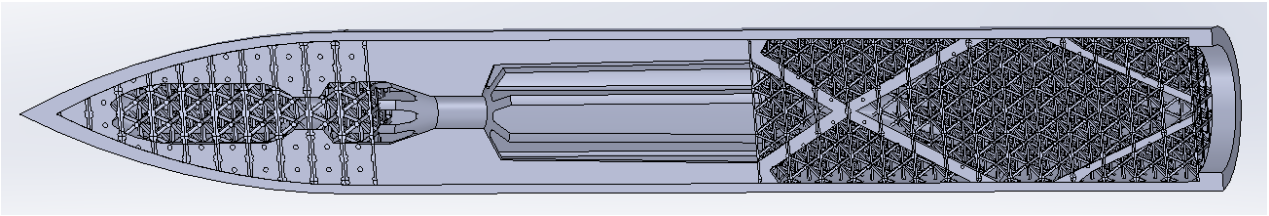

(b)

Figure 9. Example of Finished Warhead Design. *(a) Finished warhead design with outer case walls and interior solid insert. (b) Same warhead design with the addition of lattice structures for structural reinforcement.*

Of the different lattice structures presented in Figure 1(b), this warhead design utilized the microtruss lattice structure to provide good resistance to both normal and shear forces. A detailed image of the lattice structures is shown in Figure 10. However, this specific lattice structure was later determined to have printability issues and therefore later designs used the pillar textile lattice structure and slight variations thereof to minimize printability issues. This design will be slightly modified to produce the design used for actual product testing.

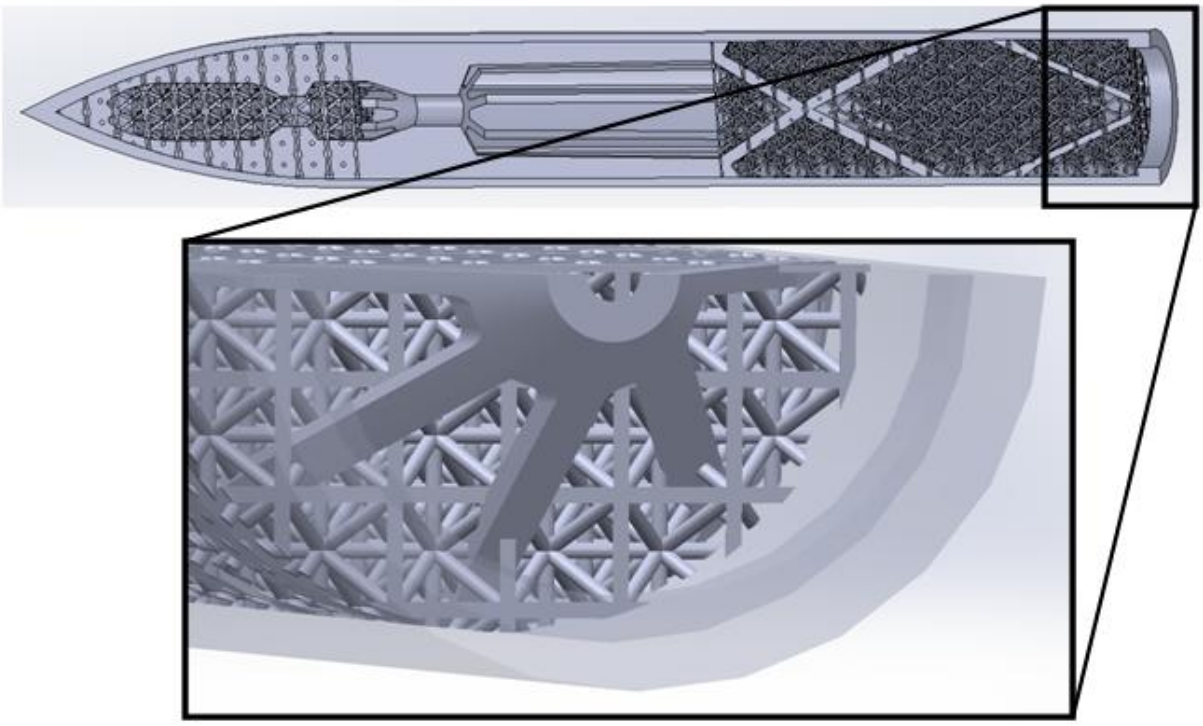

Figure 10. Finished Warhead Design, Lattice Structure Detail. *Detail of lattice structures (same warhead design as in Figure 9). Shown from tail end.*

This warhead design reflects only the process used to generate warhead designs from optimization results. It is not a printed design. This warhead had printability issues stemming from the choice of the microtruss lattice structure and the nature of the solid insert. The discovery of these issues was crucial in the learning process and will be resolved in the final design for live fire testing.

E. Printing & Testing Details

At least two, and preferably three, of both the standard and the optimized warheads will be produced in the EOS StainlessSteel PH1. When combined with the additional three Eglin steel warheads, a total of three sets of three warheads will be generated for testing. To simplify the additive manufacturing and improve finished product tolerance, the additively manufactured warheads will be fabricated with a 0.5 mm thick external jacket and no back wall. Once the builds are deemed successful, the warheads will be separated from the build plate, cleaned of excess powder, and have the jacket machined away and threads machined at the aft end of the warhead to accept an end cap made from traditionally manufactured stainless steel.

The warheads will be empirically tested at Eglin AFB, FL to demonstrate the feasibility of the topology optimized warheads and the additively manufactured material. For all tests, shown in Table 4, the warheads will be the same type utilizing the CRH = 4.5 nose shape with an outer diameter of 1.0 inches and a length-to-diameter ratio of 7.5. The velocity for the initial test was selected to simulate the impact velocity of air-dropped operational ordnance. The obliquity angle of 20º was selected based on the expected worst-case obliquity of air-dropped ordnance and was also incorporated in the optimization analysis. The target for the testing was selected by AFRL and is a contained, semi-infinite 5 ksi concrete slab. The data for the live-fire testing will also be published in subsequent work.

Table 4. Live-fire Test Matrix.

Test #	Warhead Style	Warhead Mat'l	Velocity	Obliquity	Target Style	Target Mat'l
1	D1in, L/D7.5, CRH4.5	Eglin Steel	1000 ft/s	0º	Semi-infinite contained	5 ksi concrete
2	D1in, L/D7.5, CRH4.5	AM standard	1000 ft/s	0º	Semi-infinite contained	5 ksi concrete
3	D1in, L/D7.5, CRH4.5	AM optimize	1000 ft/s	0º	Semi-infinite contained	5 ksi concrete
4	D1in, L/D7.5, CRH4.5	Eglin Steel	1000 ft/s	20º	Semi-infinite contained	5 ksi concrete
5	D1in, L/D7.5, CRH4.5	AM standard	1000 ft/s	20º	Semi-infinite contained	5 ksi concrete
6	D1in, L/D7.5, CRH4.5	AM optimize	1000 ft/s	20º	Semi-infinite contained	5 ksi concrete
7 (TBD)	D1in, L/D7.5, CRH4.5	Eglin Steel	1200 ft/s	0º	Semi-infinite contained	5 ksi concrete
8 (TBD)	D1in, L/D7.5, CRH4.5	AM standard	1200 ft/s	0º	Semi-infinite contained	5 ksi concrete
9 (TBD)	D1in, L/D7.5, CRH4.5	AM optimize	1200 ft/s	0º	Semi-infinite contained	5 ksi concrete

IV. Conclusion

The goals of this research were to demonstrate the viability of additively manufactured warheads through the design, optimization, fabrication, and testing of two warhead designs. Topology optimization and the introduction of lattice structures were applied to the research as tools to reduce penetrating warhead case wall thickness and improve fragmentation properties. Initially, a preliminary warhead was generated and printed in 15-5 PH1 stainless steel. This preliminary warhead demonstrated both the performances and limitations for additive manufacturing. While the warhead was successfully printed, its dimensions were outside the expected tolerances and it suffered from misshaping during the printing process. Lessons learned from this warhead printing were applied to subsequent warhead builds. Concurrent to the preliminary warhead production, an optimized warhead design was developed, where the optimized design was produced by reducing the wall thickness of the standard design and redistributing the material produced by this reduction throughout the case interior. HyperWorks, an FEA and topology optimization software suite, was utilized to redistribute material to minimize total warhead compliance and maximize stiffness. An initial optimized design simulation was conducted, with an axial loading condition, in which the results showed a displacement 34% less than the standard design. This initial simulation provided the confidence such optimizations could meet the research objectives of decreasing wall thickness. After the completion of the initial work, many optimization runs were performed on both 2D and 3D warhead models under a variety of loading conditions. The quality of these optimizations was measured using both qualitative and quantitative measurements. Once a satisfactory optimization was generated, the warhead was designed in accordance with the optimization using CAD software packages and then additively manufactured in EOS StainlessSteel PH1. As a comparison, standard warhead designs were produced using both additive and traditional manufacturing methods. The live-fire testing of these warheads is expected to be completed in January at Eglin AFB, FL to demonstrate the capabilities of additively manufactured penetrating warheads.

Acknowledgments

This research was sponsored by Mr. Don Littrell and Ms. Rachel Abrahams, Damage Mechanisms, Munitions Directorate, Air Force Research Laboratory and Mr. Dennis Lindell, Joint Aircraft Survivability Program Office.

References

[1] Tu, Y., and Watry, C.W., "Enhanced GBU-28 Warhead Design" AFRL/MNAC, Air Force Research Laboratory, Munitions Directorate, Eglin AFB, FL, 2002.

[2] 3DSystems, "3DS Phenix Systems Datasheet" 3D Systems, Inc., Rock Hill, SC, 2013. URL: http://www.3dsystems.com/sites/www.3dsystems.com/files/phenix-metal-3d-printers-usen.pdf [cited 30 May 2014].

[3] 3D Systems Inc. Direct metal production 3D printers. 2014. Available: http://www.3dsystems.com/sites/www.3dsystems.com/files/direct-metal-brochure-0214-usen-web.pdf.

[4] Hao, L., Raymont, D., Yan, C., Hussein, A., and Young, P., "Design and Additive Manufacturing of Cellular Lattice Structures" College of Engineering, Mathematics and Physical Sciences, University of Exeter, Exeter, United Kingdom, 2012. URL: http://www.manufacturingthefuture.co.uk/research/ [cited 29 May 2014].

[5] M. F. Ashby. The properties of foams and lattices. *Philos. Trans. A. Math. Phys. Eng. Sci. 364(1838),* pp. 15-30. 2006. . DOI: 10.1098/rsta.2005.1678 [doi].

[6] Wadley, H.N.G., "Cellular Metals Manufacturing" *Advanced Engineering Materials 2002*, Vol. 4, No. 10, 2002, pp. 726-732.

[7] M. P. Bledsoe and O. Sigmund, "Topology Optimization; Theory, Methods, and Applications," pp. 2, 2003.

[8] EOS GmbH – Electro Optical Systems, "EOS StainlessSteel PH1 for EOSINT M270" Material Data Sheet, EOS GmbH, Munich, Germany, 2008.